**The EMBO Journal** Vol.18 No.8 pp.2241–2253, 1999

# Regional specialization in human nuclei: visualization of discrete sites of transcription by RNA polymerase III

**Ana Pombo, Dean A.Jackson, Michael Hollinshead, Zhengxin Wang[1], Robert G.Roeder[1] and Peter R.Cook[2]**

Sir William Dunn School of Pathology, University of Oxford, South Parks Road, Oxford OX1 3RE, UK and [1]Laboratory of Biochemistry and Molecular Biology, The Rockefeller University, York Avenue, New York, NY 10021, USA

[2]Corresponding author
e-mail: Peter.Cook@Path.OX.AC.UK

**Mammalian nuclei contain three different RNA polymerases defined by their characteristic locations and drug sensitivities; polymerase I is found in nucleoli, and polymerases II and III in the nucleoplasm. As nascent transcripts made by polymerases I and II are concentrated in discrete sites, the locations of those made by polymerase III were investigated. HeLa cells were lysed with saponin in an improved 'physiological' buffer that preserves transcriptional activity and nuclear ultrastructure; then, engaged polymerases were allowed to extend nascent transcripts in Br-UTP, before the resulting Br-RNA was immunolabelled indirectly with fluorochromes or gold particles. Biochemical analysis showed that ~10 000 transcripts were being made by polymerase III at the moment of lysis, while confocal and electron microscopy showed that these transcripts were concentrated in only ~2000 sites (diameter ~40 nm). Therefore, each site contains approximately five active polymerases. These sites contain specific subunits of polymerase III, but not the hyperphosphorylated form of the largest subunit of polymerase II. The results indicate that the active forms of all three nuclear polymerases are concentrated in their own dedicated transcription sites or 'factories', suggesting that different regions of the nucleus specialize in the transcription of different types of gene.**

*Keywords*: α-amanitin/RNA polymerase III/tagetitoxin/transcription

## Introduction

Mammalian cells contain four different RNA polymerases defined by their characteristic locations and drug sensitivities (Chambon, 1974; Weinmann *et al*., 1975). A minor activity, which is resistant to α-amanitin, is concentrated in mitochondria, while the other three activities are all nuclear. Polymerase I (pol I) is nucleolar and resistant to α-amanitin but sensitive to low concentrations of actinomycin D; polymerase II (pol II) is nucleoplasmic and more resistant to actinomycin D but sensitive to low concentrations of α-amanitin; and polymerase III (pol III) is nucleoplasmic and inhibited by high concentrations of α-amanitin.

Nucleolar sites of pol I activity have been studied in detail (Shaw and Jordan, 1995). In electron micrographs, the nucleolus has a well-defined ultrastructure; pale fibrillar centres are surrounded by the dense fibrillar component, and both are embedded in a granular component. Active polymerases are found at the interface between the fibrillar centre and dense fibrillar component, nascent transcripts in the dense fibrillar component and maturing ribosomes in the surrounding granular component (e.g. Hozak *et al*., 1994). A nucleolus can be likened to an industrial park dedicated to the production of ribosomes; 45S rRNA is made in 'factories' on the surface of fibrillar centres and assembled into ribosomes in the granular component.

The finding that pol I is concentrated within a discrete nucleolar compartment begs the question: are active forms of pols II and III also concentrated in discrete, perhaps different, nucleoplasmic compartments? In principle, it should be a simple matter to answer this question, as various approaches are available to label transcription sites. In one, living or permeabilized cells are allowed to make RNA for a short period in the presence of modified precursors (e.g. [$^3$H]U, Br-U, Br-UTP or biotin-CTP); then, incorporated analogues are detected by autoradiography or immunolabelling (Fakan *et al*., 1976; Jackson *et al*., 1993, 1998; Wansink *et al*., 1993; Hozak *et al*., 1994; Iborra *et al*., 1996). In a second, polymerases or their associated transcription factors are immunolocalized (e.g. Bregman *et al*., 1995; Grande *et al*., 1997; Kim *et al*., 1997; Pombo *et al*., 1998). In practice, several interrelated factors complicate analysis of pol III sites. First, the major pol III transcripts, i.e. 5S rRNA and the tRNAs, have lengths of only 120–121 and 75–95 nucleotides, respectively (Geiduschek and Tocchini-Valentini, 1988), and this short length inevitably makes detection difficult. Secondly, these short transcripts are made quickly, so precursors such as [$^3$H]U and Br-U must be transported through membranes, converted into immediate precursors and equilibrated with internal pools before they can be incorporated into nascent RNA. While permeabilization allows direct access of precursors such as Br-UTP and biotin-CTP and control over elongation rates, the conditions used could disturb nuclear organization. Thirdly, the transcripts are both made and exported rapidly from synthetic sites; as a result, concentrations of transcripts detected by *in situ* hybridization (e.g. Matera and Ward, 1993; Matera *et al*., 1995) generally mark distant downstream sites. Fourthly, it is difficult to localize precisely the incorporated labels; after autoradiography, silver grains may be hundreds of nanometres away from incorporated $^3$H, and immunolabelling gold particles can lie 20 nm away from the Br-RNA or biotin-RNA they mark (Griffiths, 1993; Iborra and Cook, 1998). Fifthly, polymerases and their

transcription factors are often stored in certain parts of the nucleus, but used in others; as a result, the most intensely labelled sites are often inactive (e.g. Grande *et al*., 1997).

Despite these difficulties, Fakan and colleagues localized nucleoplasmic transcription sites after incubating cells with [$^3$H]U for as little as 2 min; they found silver grains in autoradiographs over perichromatin fibrils at the edge of condensed chromatin (e.g. Fakan and Puvion, 1980; reviewed by Fakan, 1994). More recently, 500–8000 nucleoplasmic 'foci' or 'factories' where Br-UTP and biotin-CTP are incorporated have been visualized by immunofluorescence and high-resolution electron microscopy (Jackson *et al*., 1993; Wansink *et al*., 1993; Iborra *et al*., 1996, 1998; Fay *et al*., 1997). As labelling was sensitive to a low concentration of α-amanitin, these represent sites of pol II activity; however, no pol III sites were detected (Jackson *et al*., 1993; Wansink *et al*., 1993; Zeng *et al*., 1997). One study suggests that pol III sites are distinct from pol II sites; α-amanitin reduces the number of transcription sites detected in cells infected with adenovirus (Pombo *et al*., 1994).

We now characterize pol III sites in uninfected cells. Cells are lysed with saponin in a buffer that preserves transcriptional activity and nuclear ultrastructure; then, nascent transcripts are extended in Br-UTP, and the resulting Br-RNA is immunolabelled with fluorochromes or gold particles. In a HeLa cell, we find that ~10 000 transcripts are being made by pol III at any moment, and that these transcripts are concentrated in ~2000 sites with a diameter of ~40 nm. These sites are sensitive to high concentrations of α-amanitin that inhibit pol III, and contain pol III-specific subunits, but not the hyperphosphorylated form of the largest subunit of pol II. Just as pol I is concentrated in a discrete (nucleolar) compartment, our results suggest that the active forms of pols II and III are also concentrated in their own dedicated 'factories' in the nucleoplasm.

## Results

### *Establishing conditions for the detection of pol III transcripts*

In order to visualize nascent pol III transcripts, we improved a procedure known to preserve considerable polymerizing activity and structure (Jackson *et al*., 1993). HeLa cells were encapsulated in agarose microbeads to protect them, and lysed with saponin in a 'physiological' buffer (PB). Then, [$^{32}$P]UTP is incorporated efficiently into RNA (Figure 1A, curve 1). Addition of 100 mg/ml polyethylene glycol (not shown) or sucrose increases incorporation slightly (Figure 1A, curve 2). Addition of bovine serum albumin (BSA) (giving PB-BSA) further increases incorporation (Figure 1A, curve 3), but excess saponin then reduces it (Figure 1A, curve 4). Conditions giving maximum incorporation were used subsequently. Electron microscopy showed that these conditions preserved ultrastructure better than those used before (Figure 2). For example, electron density and fine structure in nuclei remain more like those seen in unlysed controls. Mitochondrial structure also survives, and probably underlies the preservation of transcriptional activity in this organelle (see below). These results show that gross activity and ultrastructure are well preserved under these conditions.

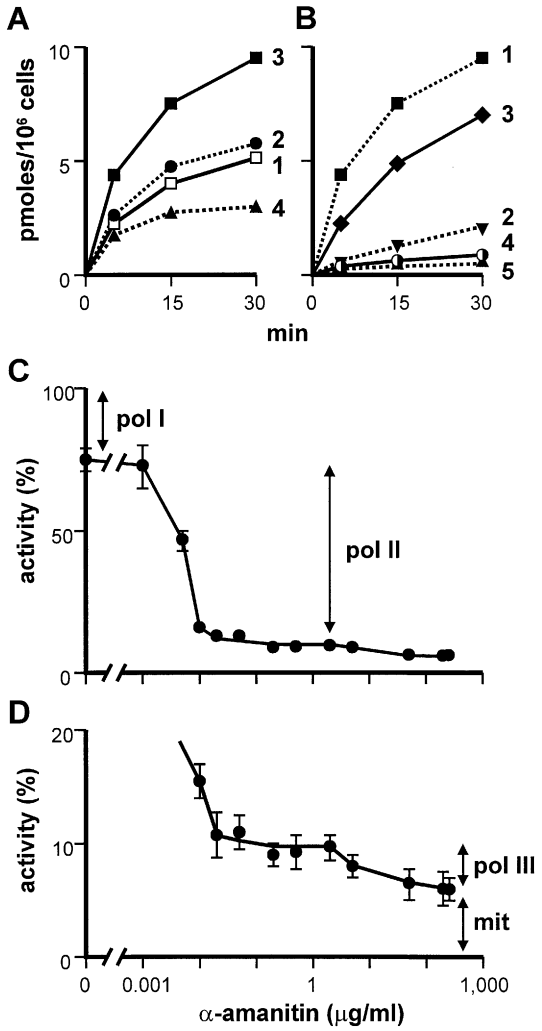


**Fig. 1.** Transcription by pol III. Encapsulated HeLa cells were lysed, allowed to extend nascent transcripts in [$^{32}$P]UTP, and the pmoles of UMP incorporated/$10^6$ cells were determined. (**A**) Effect of lysis and elongation buffers. Curve 1: lysis in PB + 0.5 mg/ml saponin, elongation in PB. Curve 2: as curve 1, but 100 mg/ml sucrose was present during lysis and elongation. Curve 3: lysis in PB-BSA + 1 mg/ml saponin, elongation in PB-BSA. Curve 4: lysis in PB-BSA + 3 mg/ml saponin, elongation in PB-BSA. (**B**) Effect of inhibitors. Cells were grown with or without 0.2 μg/ml actinomycin D for 15 min, lysed in PB-BSA + 1 mg/ml saponin, resuspended in PB-BSA and allowed to extend nascent transcripts with or without α-amanitin. Curve 1: no drugs added. Curve 2: + 250 μg/ml α-amanitin to inhibit pols II and III. Curve 3: + actinomycin to inhibit pol I. Curve 4: + actinomycin, + 2 μg/ml α-amanitin to inhibit pols I and II. Curve 5: + actinomycin, + 250 μg/ml α-amanitin to inhibit pols I, II and III; mitochondrial synthesis remains. (**C** and **D**) The effect of α-amanitin (plotted on a logarithmic scale). Cells were grown in 0.2 μg/ml actinomycin for 15 min prior to lysis (to inhibit pol I), lysed in PB-BSA + 1 mg/ml saponin, resuspended in PB-BSA and allowed to extend nascent transcripts in 0–250 μg/ml α-amanitin. Transcription rates (determined as for B, curves 3, 4 and 6) were expressed as a percentage of the rate given by cells treated without drugs. Some data in (C) are reproduced in (D) using an expanded scale. Error bars show ±SD (from two-to-five experiments).

We next determined the maximum concentration of α-amanitin that inhibited pol II but left pol III unaffected. A typical experiment is illustrated in Figure 1B, and the results are summarized in Figure 1C and D. A

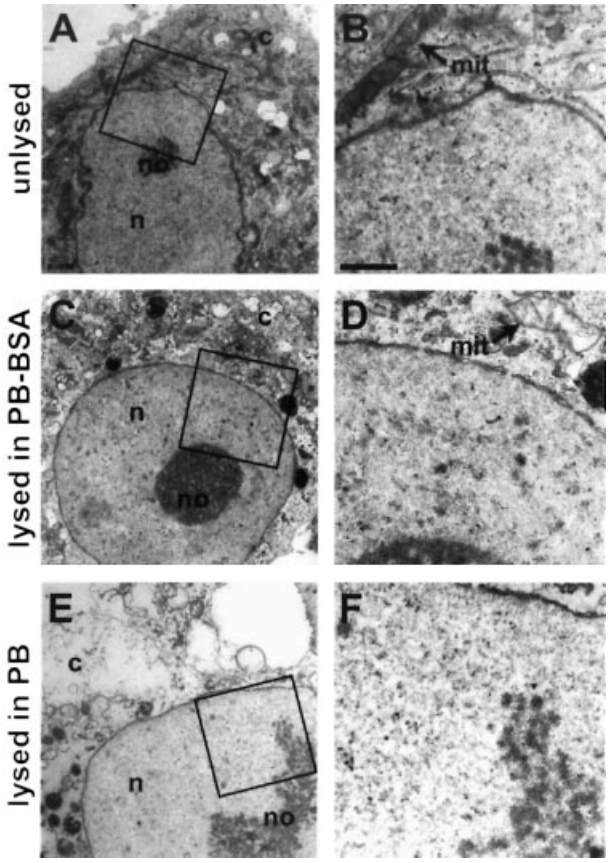


**Fig. 2.** Comparison of cellular ultrastructure after lysis in PB-BSA and PB. Cells were treated variously, fixed and electron micrographs of thin sections collected; regions in the rectangles are shown enlarged on the right. c, cytoplasm; mit, mitochondrion; n, nucleoplasm; no, nucleolus. Bars = 1 μm. (**A** and **B**) Unlysed cells. (**C** and **D**) Lysis in PB-BSA. The plasma membrane and most cytoplasmic components remain, although mitochondria swell; this is due mainly to incubation at 4°C, rather than to the effects of saponin (not shown). The texture of the nucleus remains unchanged, although some material is extracted. (**E** and **F**) Lysis in PB. The plasma membrane, cytoplasm and mitochondria all appear extracted; the nucleoplasm also appears more extracted, and its texture is altered.

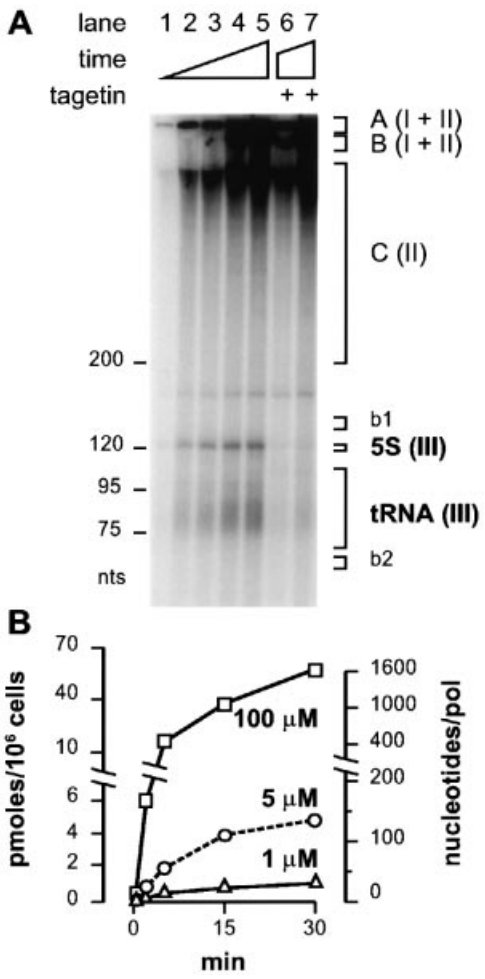


**Fig. 3.** Transcript profiles. (**A**) Nascent transcripts were extended for 0.25 (lane 1), 2 (lane 2), 5 (lane 3), 15 (lanes 4 and 6) or 30 min (lanes 5 and 7) in 100 μM Br-UTP ± 20 μM tagetitoxin (tagetin) and a trace of [$^{32}$P]UTP; then, [$^{32}$P]RNA from equal numbers of cells was loaded on each lane in a gel, an autoradiogram prepared and the intensities in the various zones measured. The polymerase making most transcripts in each zone was deduced using inhibitors and is indicated in parentheses. A concentration of 2 μg/ml α-amanitin reduced the intensities of zones A, B and C to 27, 26 and 7%, without effect on the 5S or tRNA zones; 200 μg/ml eliminated all labelling above background that was detectable in the 5S and tRNA zones (not shown). In lane 7, tagetitoxin reduced the intensities in zones A, B and C, 5S and tRNA to 100, 96, 98, 16 and 12% of those seen in lane 5. Zones b1 and 2 were used for background subtraction. nts: length in nucleotides. (**B**) Incorporation (pmol of UMP) in 1–100 μM Br-UTP. The number of nucleotides incorporated per polymerase (assuming 90 000 active polymerases/nucleus and no termination or reinitiation) is indicated on the right.

concentration of 0.2 μg/ml actinomycin D inhibits pol I (Figure 1C). Use of such a high concentration ensures that essentially all pol I is inhibited (see below), while incorporation into 5S and tRNA is reduced by only 7 and 4%, respectively (determined using autoradiographs like that shown in Figure 3A; not shown). Addition of α-amanitin progressively inhibits pol II, until concentrations between 0.1 and 2 μg/ml have no further effect (Figure 1C). Therefore, 2 μg/ml α-amanitin was used to inhibit pol II, and to leave pol III activity. This concentration is 15-fold higher than that required to inhibit pol II, but it has a negligible effect on pol III. Pol III activity was then abolished by 250 μg/ml α-amanitin, leaving the resistant mitochondrial activity (Figure 1D). This inhibition profile is like that seen with pure polymerases *in vitro* (e.g. Weinmann *et al*., 1975; Weil and Blatti, 1976).

The effects of these inhibitors are additive. Thus, 25 ± 4% (pol I) activity is inhibited by 0.2 μg/ml actinomycin (Figure 1C), and 27 ± 3% (pol I plus mitochondrial) activity resists 250 μg/ml α-amanitin (e.g. Figure 1B, curve 2). These percentages are similar to those seen previously in HeLa cells (e.g. McReynolds and Penman, 1974; Udvardy and Seifart, 1976; Weil and Blatti, 1976).

### *Number of engaged pol III complexes per cell*

We next determined how many molecules of pol III are active at any moment in a HeLa nucleus. The number can be estimated if 5% of the total activity is due to pol III (Figure 1B and C) and a typical cell contains ~90 000 nascent transcripts (Jackson *et al*., 1998); then, ~4500 pol III complexes would be active (Figure 1). However, this crude estimate takes no account of differences in elongation rate, transcript length or rates of initiation and termination by the different polymerases. Therefore, we

estimated the number of pol III complexes more precisely using a strategy that does not rely on the use of α-amanitin and actinomycin. The approach depended on the shortness and defined length of the principal pol III transcripts, which enable them to be resolved by gel electrophoresis. Transcription reactions were carried out in the presence of Br-UTP, which has no detectable effect on pol III activity (see Materials and methods); therefore, the same conditions could be used for microscopy. [Similar results were obtained when UTP replaced Br-UTP (not shown).] Nascent transcripts were extended for different periods in the presence of Br-UTP plus a trace of [$^{32}$P]UTP, run on a gel and visualized by autoradiography (Figure 3A, lanes 1–5). The longest transcripts (made by pols I and II) either remained at the origin (zone A) or ran a short way into the gel (zones B and C). However, pol III transcripts ran well into the gel; completed 5S rRNA formed a sharp band of 120–121 nucleotides, and completed tRNAs a smear between 75 and 95 nucleotides. These assignments were confirmed using α-amanitin and actinomycin (not shown); for example, 200 μg/ml α-amanitin abolished all detectable labelling in the 5S rRNA band and tRNA smear (not shown). Reducing the concentration of Br-UTP from 100 to 1 μM reduced the amount of RNA made (Figure 3B).

Next, we investigated whether pol III reinitiated using two different inhibitors. Kovelman and Roeder (1990) used 0.05% sarkosyl to prevent reinitiation by the pure enzyme, but no 5S rRNA and tRNA bands could be detected in this complex system, despite increased incorporation by pols I and II (not shown). The second inhibitor, tagetitoxin (tagetin; Steinberg *et al*., 1990), proved more useful, even though its effects are complex. The extent of inhibition depends on nucleotide concentration, type of pol III transcription unit (Steinberg and Burgess, 1992) and enzyme purity (Kock and Cornelissen, 1991). However, the inhibitor efficiently stalls yeast pol III at pause sites on 5S and tRNA genes (Steinberg and Burgess, 1992), but allows pre-engaged mammalian polymerases to complete the first round of synthesis, while preventing subsequent rounds (Maraia *et al*., 1994). Under efficient transcription conditions, an inhibitor that prevents recycling should allow a pre-engaged polymerase to complete synthesis of its transcript, but prevent synthesis of additional ones; under less efficient conditions, it would have little effect as so few first transcripts are completed. We found that in 100 μM Br-UTP, tagetitoxin reduced incorporation in the 5S and tRNA regions (Figure 3A, compare lanes 4 with 6, and 5 with 7; Table I), but in 1 μM Br-UTP it had little effect (Table I). These results suggest that the drug limits synthesis to one round in 100 μM Br-UTP, but in 1 μM Br-UTP so few nucleotides are added that most polymerases do not complete synthesis of the first transcript. The number of transcripts completed by pol III can be calculated (see Materials and methods), as specific activities, cell numbers, loadings per lane and amount of label per transcript are all known. In 100 μM Br-UTP and tagetitoxin (i.e. under conditions where polymerases have ample time to complete the first transcript but cannot initiate new ones), ~1400 5S and ~6500 tRNA transcripts are made (Table I). As other transcripts are made by pol III (e.g. U6, MRP, 7SK, 7SL and RNase P RNAs), perhaps ~10 000 pol III complexes are active. In the absence of tagetitoxin, three-to-five times this number of transcripts are made, as new ones are initiated.

**Table I.** Extent of transcription *in vitro*

| | 1 μM Br-UTP | | 100 μM Br-UTP | |
|---|---|---|---|---|
| | 5S rRNA | tRNA | 5S rRNA | tRNA |
| Fraction total intensity (%) | | | | |
| −tagetitoxin | 0.41 | 2.7 | 0.52 | 2.3 |
| +tagetitoxin | 0.39 | 2.4 | 0.055 | 0.18 |
| Nucleotides×$10^{-6}$/cell | | | | |
| −tagetitoxin | 0.010 | 0.063 | 0.51 | 2.3 |
| +tagetitoxin | 0.009 | 0.050 | 0.080 | 0.28 |
| Completed transcripts/cell | | | | |
| −tagetitoxin | 170 | 1500 | 4900 | 30 000 |
| +tagetitoxin | 150 | 1200 | 1400 | 6500 |

Nascent transcripts were extended for 15 min in 1 or 100 μM Br-UTP ± 20 μM tagetitoxin and a trace of [$^{32}$P]UTP, run on a gel, an autoradiograph prepared (as in Figure 3A), and the intensities in the 5S rRNA and tRNA zones expressed as a fraction of the total intensity in the lane. The number of nucleotides incorporated into these transcripts and the number of transcripts completed by each cell were then calculated (see Materials and methods).

### *Visualizing nascent transcripts made by the different polymerases*

We next visualized nascent RNA made by the different polymerases. Permeabilized cells were allowed to make RNA under conditions in which pols I and II extend nascent transcripts by ~1000 nucleotides, and each pol III completes three-to-five transcripts (Figure 3B; Table I); then, sites containing Br-RNA were immunolabelled indirectly with Cy3 and imaged in a 'confocal' microscope. In Figure 4A–H, single optical sections through the centre of nuclei illustrate distributions of nucleic acids (TOTO-3 fluorescence) and Br-RNA. In the absence of drugs, discrete foci containing Br-RNA are seen in nucleoli, the nucleoplasm and cytoplasm (Figure 4B). This pattern is generally similar to that seen previously (Jackson *et al*., 1993; Wansink *et al*., 1993; Iborra *et al*., 1996; Fay *et al*., 1997), except that these conditions preserve cytoplasmic (i.e. mitochondrial) foci, and >95% cells in the population have a similar appearance. [Using these improved conditions, variations in transcriptional activity of the type seen by Zeng *et al*. (1997) are not observed.] If pol II is inhibited, the number of nucleoplasmic foci falls, to leave pol III foci (Figure 4D). Inhibiting both pols II and III abolishes all nucleoplasmic labelling, but leaves nucleolar and mitochondrial foci (Figure 4F). Actinomycin D affects the number and intensity of the various foci in different ways; for example, 0.05, 0.1 and 0.2 μg/ml actinomycin D progressively decreases the number of cells containing nucleolar foci to 20, 5 and 0% (not shown).

Modern 'confocal' microscopes have, at best, a resolution of ~200, ~200 and ~500 nm in the *x*-, *y*- and *z*-axes, respectively (Pawley, 1995). Two reasons make it difficult to count individual foci within sections such as those in Figure 4B. First, the faint foci seen could result either from low concentrations of Br-RNA lying in the plane of the section or from out-of-focus flare from high concentrations lying hundreds of nanometres above or below.

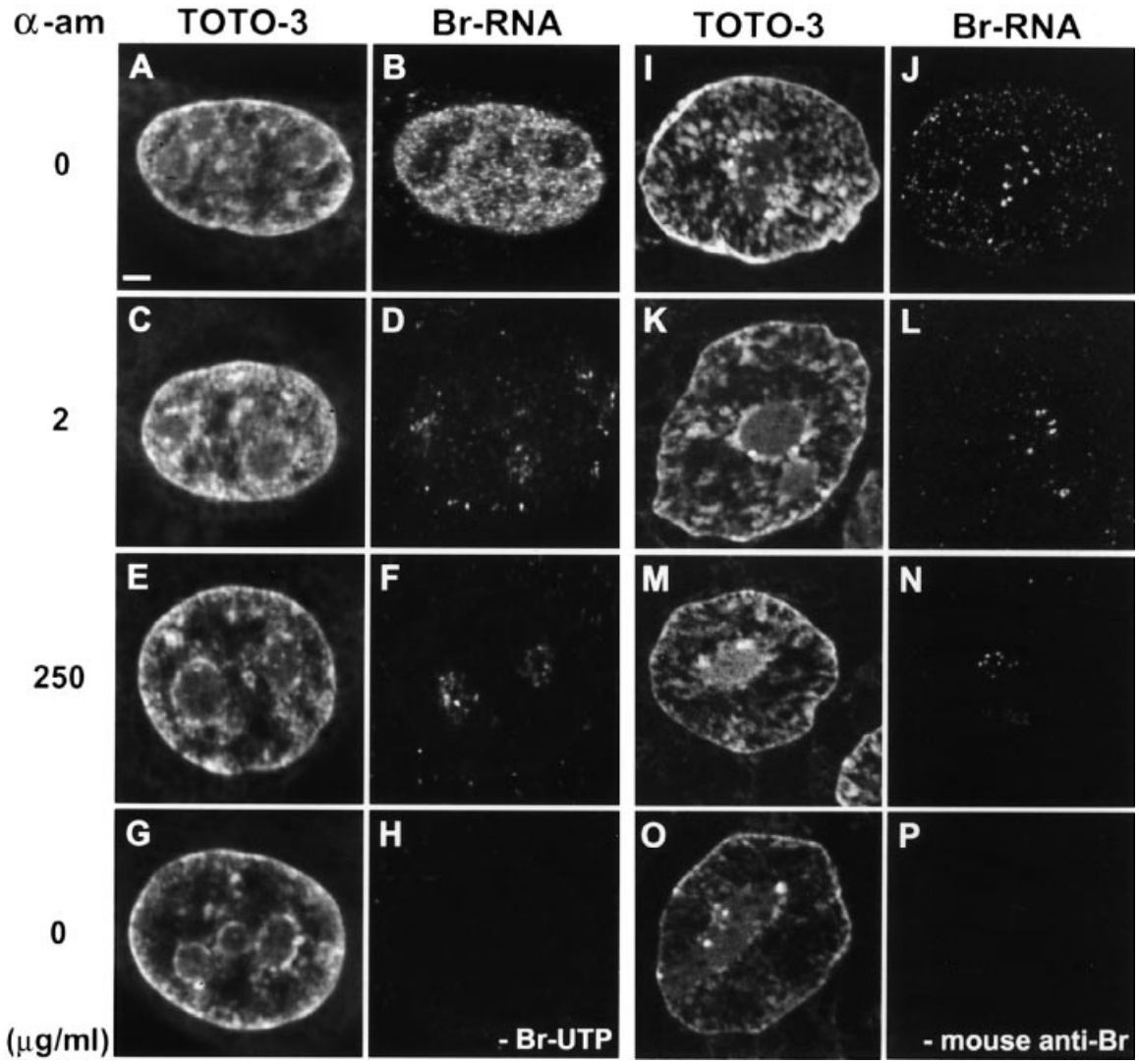


**Fig. 4.** Nascent pol III transcripts in (A–H) whole cells or (I–P) cryosections. Nascent transcripts were extended (100 μM Br-UTP; 15 min) with or without α-amanitin as indicated, sites containing Br-RNA were immunolabelled indirectly with Cy3 (nucleic acids were counterstained with TOTO-3), and red and far-red images of one optical section were collected using a 'confocal' microscope; pairs of images are shown without background subtraction (thresholding). (A–H) show equatorial sections selected from stacks of images through whole cells, while (I–P) are views of individual cryosections of ~90 nm. Bar = 2.5 μm. (**A** and **B**) Foci containing Br-RNA are seen in nucleoli, the nucleoplasm and mitochondria. (**C** and **D**) Sufficient α-amanitin to inhibit pol II reduces the density of nucleoplasmic foci, without affecting nucleolar or mitochondrial foci. (**E** and **F**) A concentration of 250 μg/ml α-amanitin inhibits pols II and III, and abolishes nucleoplasmic labelling (but not nucleolar or mitochondrial foci). (**G** and **H**) Essentially no labelling is seen when Br-UTP is omitted. (**I** and **J**) Fewer, more discrete, Br-RNA foci of all types are seen in cryosections. (**K** and **L**) When pol II is inhibited, only a few pol III foci are seen in the nucleoplasm. (**M** and **N**) When pols II and III are inhibited, no nucleoplasmic foci are seen. (**O** and **P**) Essentially no labelling is seen when the primary antibody is omitted.

Although resolution can be improved by deconvoluting information from serial sections, this brings attendant problems (e.g. Pawley, 1995). Secondly, many foci appear to merge one into another in the thick section, and these will be resolved better the thinner the section. Imaging (cryo)sections ~100 nm thick provides an alternative and direct way of improving *z*-axis resolution (Figure 4I–P); then, much more detail is seen in the TOTO-3 images (compare Figure 4A with I), and, most importantly, fewer, sharper, foci are seen (compare Figure 4B with J). [See Pombo *et al*. (1999) for a discussion of the improved resolution given by cryosectioning.] A concentration of 2 μg/ml α-amanitin reduces the number of nucleoplasmic foci to one-fifth (Figure 2D and L), leaving (pol III) foci which are about one-third as intense as the pol II foci (not shown). A concentration of 250 μg/ml α-amanitin eliminates all nucleoplasmic foci to leave only nucleolar and cytoplasmic (mitochondrial) foci (Figure 4F and N). No foci are seen in the nucleus or cytoplasm when Br-UTP or the primary antibody is omitted (Figure 4H and P), or after RNase treatment (1 mg/ml for 1 h at 37°C; not shown); therefore, they contain Br-RNA. These results are consistent with the nucleoplasm containing two populations of foci, with four-fifths being sensitive to 2 μg/ml α-amanitin (and so due to pol II), and one-fifth being resistant to 2 μg/ml α-amanitin but sensitive to 250 μg/ml (and so due to pol III).

As the true dimensions of sites <200 nm cannot be determined by light microscopy, and as transcription sites often lie within 200 nm of each other (Iborra *et al*., 1996), we imaged transcription sites by electron microscopy; Br-RNA in the cryosections was immuno-

**Table II.** Density of transcription sites in the nucleoplasm

| Conditions | Particles per cluster | Clusters per $\mu m^2$ |
|---|---|---|
| Pol II + III (no α-amanitin) | | |
| 1. 100 μM Br-UTP, 15 min | 8 | 2.2 |
| Pol III (2 μg/ml α-amanitin) | | |
| 2. 100 μM Br-UTP, 15 min [1×] | 6 | 0.55 |
| 3. 100 μM Br-UTP, 2 min [0.15×] | 6 | 0.49 |
| 4. 5 μM Br-UTP, 15 min [0.1×] | 5 | 0.36 |
| Controls | | |
| 5. As 1, plus 250 μg/ml α-amanitin | 3 | 0.1 |
| 6. As 1, no Br-UTP | 2 | 0.2 |
| 7. As 1, no anti-Br antibody | 0 | 0.0 |
| 8. As 1, RNase treated (1 mg/ml; 2 h; 37°C) | 2 | 0.1 |

Nascent transcripts were extended in Br-UTP and sites containing Br-RNA labelled with gold particles; then, images like those in Figure 5 were collected, and the numbers of lone and clustered gold particles counted. Results are shown for one typical experiment using cryosections of ~90 nm. For each row: (i) 33–110 images from >33 randomly selected cells were counted so that values given by the last 10% analysed changed the progressive mean value of the number of clusters/$\mu m^2$ by <10%; and (ii) there were ⩽0.9 lone particles/$\mu m^2$ due to background (rows 1–8 gave 0.7, 0.2, 0.2, 0.3, 0.9, 0.6, 0.06 and 0.7 lone particles/$\mu m^2$, respectively). In rows 1–4, lone particles accounted for ⩽8% of all particles. Relative incorporation rates, shown in square brackets, were obtained from Figure 3B.

labelled indirectly with gold particles, and the sections stained with uranyl acetate. Only ⩽8% gold particles were found alone over the nucleoplasm; the rest were in clusters (see legend in Figure 5 and Table II footnotes). The lone particles represent background labelling, as the same numbers are seen if: (i) cells are incubated with 250 μg/ml α-amanitin; (ii) Br-UTP or the primary antibody are omitted; or (iii) sections are incubated with RNase prior to immunolabelling (Table II, lines 5–8; see also Iborra *et al*., 1996). The clusters mark Br-RNA as they are removed by RNase treatment (Table II, line 8). After synthesis in the absence of α-amanitin (Figure 5A), many clusters are over the nucleoplasm (small circles), nucleoli (large circles) or cytoplasm (not shown). Inhibiting pol II reduces the number of nucleoplasmic clusters to one-fifth, without effect on the nucleolar clusters (Figure 5B). The results confirm those obtained by light microscopy (Figure 4). The nucleoplasmic clusters seen in the presence of 2 μg/ml α-amanitin generally had similar ultrastructures to those seen in the absence of the drug (compare Figure 5C and D); this suggests that pols II and III sites have similar structures. Most (pol III) clusters seen in 2 μg/ml α-amanitin were found alone (Figure 5B). However, a few were grouped in pairs (Figure 5D) and, rarely (about once every 500 $\mu m^2$), more complex groups were seen (Figure 5E); these rare pairs/groups could reflect transcripts encoded by tandemly arranged genes.

### *Numbers of pol III sites*

The total number of the different kinds of sites in a HeLa cell nucleus can be estimated (using standard stereological techniques; Materials and methods) from the densities in sections of known thicknesses, site diameter and nuclear volume. Therefore, we measured each in turn. Site numbers were counted in images obtained by confocal microscopy of whole cells or cryosections (not shown), and by electron microscopy of cryosections. The results obtained with the latter technique are given, as it provides the highest resolution and equivalent sensitivity. [Pombo *et al*. (1999) discuss the advantages and disadvantages of the different approaches, and show that they reveal exactly the same sites.] For this analysis, we define a cluster of gold particles as one containing more than one particle lying within 40 nm of another (centre–centre distance). [Approximately 40 nm is the maximum separation possible between two particles marking adjacent bromine residues in a transcript (i.e. roughly the length of two fully extended immunolabelling probes, each containing two immunoglobulins and a protein A molecule).] In the absence of α-amanitin, there were 2.2 nucleoplasmic clusters/$\mu m^2$, which typically contained eight particles (Table II, row 1). Most of these clusters marked pol II + III sites, while a few (i.e. 0.2 clusters/$\mu m^2$) with only two particles represented background (Table II, rows 5–8). In 2 μg/ml α-amanitin, there were only 0.55 clusters/$\mu m^2$ with six particles per cluster (Table II, row 2), against the same background.

Despite the sensitivity of the technique, it remained possible that some pol III sites went undetected, perhaps because they contained too little bromine. If so, increased bromine content should allow more undetected sites to be detected. However, varying the amount of incorporation over a 10-fold range, which was achieved using different Br-UTP concentrations and incorporation times, had only a marginal effect on cluster density (Table II, rows 2–4). These results are consistent with most pol III sites being detected.

Next, we determined the size of transcription sites using a method that allows the radii of spheres to be deduced from the radii of circular profiles seen in two-dimensional images of three-dimensional sections cut through the sample. Sites containing Br-RNA made by pols II + III and pol III had corrected radii of 23 ± 3 and 20 ± 2 nm, respectively (Figure 6).

We went on to calculate the number of sites in a typical nucleus from the site density (Table II), diameter (Figure 6) and nucleoplasmic volume (Materials and methods). Thus, 2.2 clusters/$\mu m^2$ marked nucleoplasmic sites containing Br-RNA made by pols II + III (Table II, row 1), of which 0.2 were due to background (Table II, row 6); the 2 clusters/$\mu m^2$ above background corresponds to ~9700 nucleoplasmic sites in a nucleus. Similarly, 0.35 clusters/$\mu m^2$ marked pol III sites (from Table II, rows 2 and 6), equivalent to 1800 sites per nucleus. As cells contain more active polymerizing complexes than sites, it follows that each site must contain more than one polymerase. Furthermore, as a pol III transcription unit of ~100 nucleotides is unlikely to be associated with more than one engaged polymerase (e.g. Braun *et al*., 1989; Bartholomew *et al*., 1993), it also follows that each site must contain more than one active transcription unit.

### *Pol III and its transcripts are found in dedicated sites*

As each site contains more than one polymerase, are pols II and III active in the same site, or is each polymerase found in its own distinct site? If the different polymerases were intermingled within one site, and if most sites were detected, we would expect 2 μg/ml α-amanitin to reduce the intensity of labelling within a site without much effect

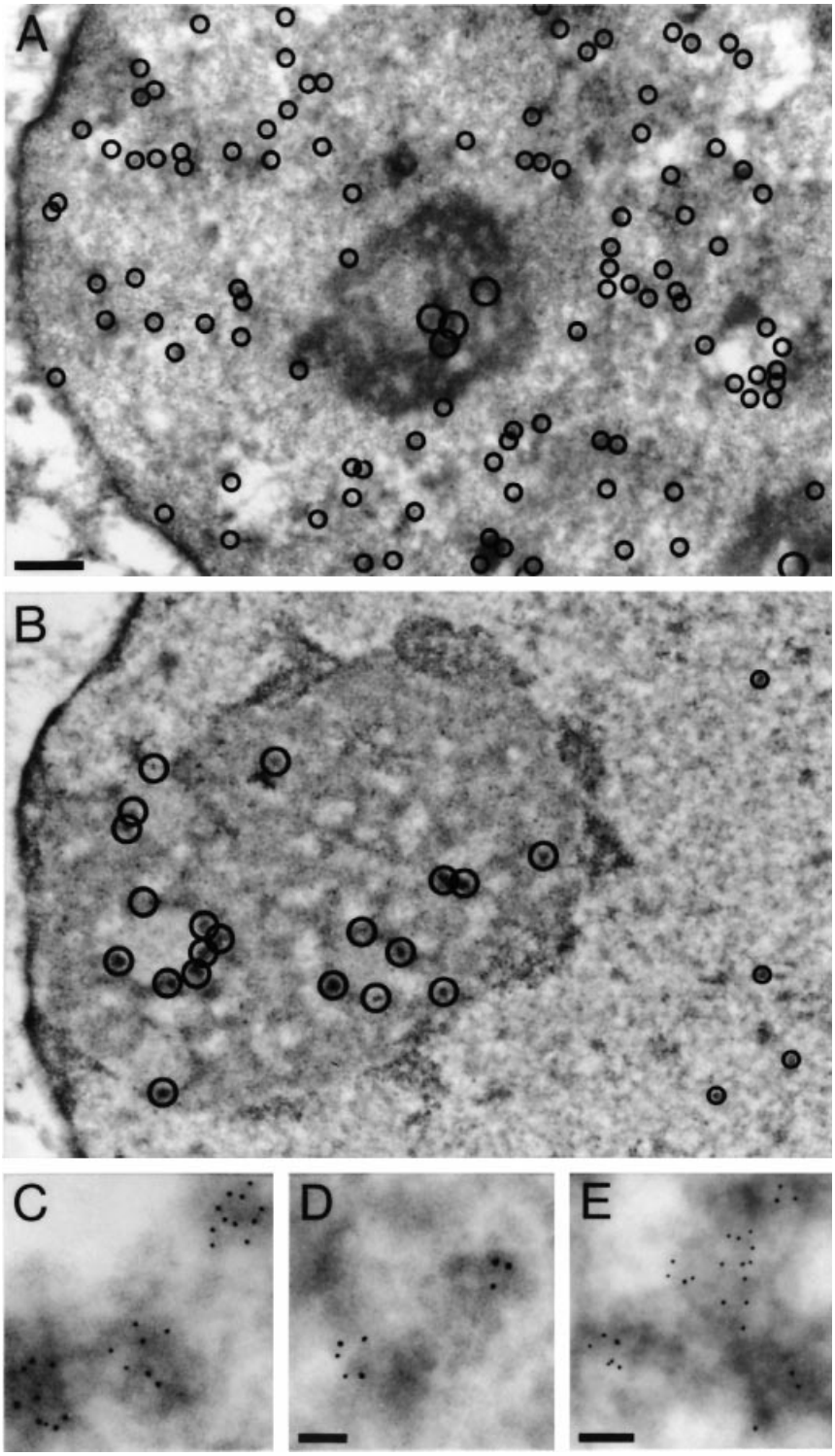


**Fig. 5.** Transcription sites imaged by electron microscopy of cryosections. Nascent transcripts were extended (100 μM Br-UTP; 15 min) with or without 2 μg/ml α-amanitin; after fixation and cryosectioning, sites containing Br-RNA were immunolabelled indirectly with gold particles (5 nm), stained with uranyl acetate and imaged. Bars = 500 nm (A and B), 50 nm (C and D) and 75 nm (E). (**A**) Gold particles marking Br-RNA are concentrated in 102 nucleoplasmic clusters (small circles; each typically contains 11 particles). Five clusters (large circles) are also seen over the two nucleoli. Twenty-six and three lone particles lay over the nucleoplasm and nucleoli, respectively. (**B**) After extension in 2 μg/ml α-amanitin, nucleoplasmic labelling is concentrated in only four clusters (small circles; each typically contains eight particles); nucleolar clusters (large circles) are unaffected. Six and four lone particles lay over the nucleoplasm and nucleoli, respectively. (**C**–**E**) High-power views of typical clusters after extension without (C) and with 2 μg/ml α-amanitin (D and E); they have similar ultrastructures, but those in α-amanitin are usually marked by fewer particles.

on site density. On the other hand, if the two polymerases were concentrated in their own dedicated sites, inhibition of pol II activity should leave only the pol III sites. Results were consistent with this second possibility; site density was reduced to one-fifth (Figure 4; Table II).

We went on to see if pol II was not generally found

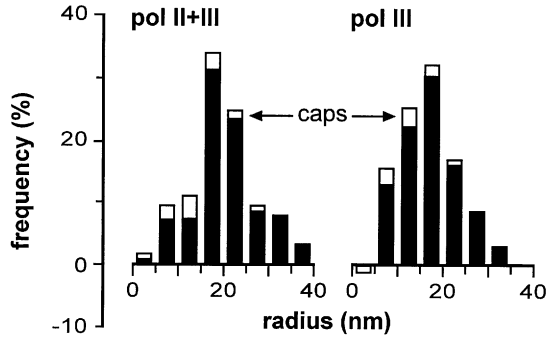


**Fig. 6.** The radii of transcription sites. The (three-dimensional) radii of the spheres underlying the (two-dimensional) clusters of gold particles such as illustrated in Figure 5C and D were deduced using the 'sequential subtraction method' (Weibel, 1979, 1980; Materials and methods). Spheres lying completely within a section appear as circles with the true radius; any cut non-equatorially may give 'polar caps' that either appear smaller, or are missed because they are too small to be detected. The method allows corrections to be made so that the true size can be determined. Radii of >65 clusters of gold particles were measured and grouped together into bins (0–5 nm, 5–10 nm, etc.). Starting with the largest bin, the contribution of polar caps arising from spheres with this radius is calculated, and subtracted from the smaller categories; then, the next largest bin is treated in the same way, and so on. White rectangles reflect the contribution of polar caps, and black rectangles the corrected frequencies. Clusters marking RNA made by pols II + III and III had weighted mean radii of 23 ± 3 and 20 ± 2 nm, respectively; this difference was not significant ($P > 0.05$, Kolmogorov–Smirnov statistical test). For pol III, negative frequencies reflect caps arising from larger spheres that must have been present, but which went undetected.

near pol III transcripts, nor pol III near pol II transcripts. Several factors complicate the analysis. First, nuclei contain pools of inactive polymerases far from transcription sites (e.g. Iborra *et al*., 1996). Fortunately, an antibody is available that detects the hyperphosphorylated form of the largest subunit of pol II (i.e. $II_O$; Bregman *et al*., 1995; Kim *et al*., 1997) that has been implicated in active transcription (Dahmus, 1996). Secondly, quantitative analysis of co-localization within sites only ~40 nm across is bedevilled by steric hindrance between probes with diameters of ⩾20 nm. Thus, Br-RNA is detected optimally here with three IgGs (each with a length of ~9 nm) and 5 nm gold particles (Materials and methods), while pol $II_O$ is detected with the H5 antibody (an IgM of ~20 nm diameter). Indeed, inclusion of the anti-pol $II_O$ antibody when labelling Br-RNA led to the detection of 25% fewer Br-RNA sites (not shown), showing that it did prevent access of the anti-Br-dU antibody to its target. Nevertheless, these experiments also gave the following results. First, pol $II_O$ and pol III often lay immediately next to their own transcripts (Figure 7A and B). Secondly, only 12% of sites containing pol III transcripts lay within 30 nm of a pol $II_O$ site (not shown). Thirdly, the presence of pol $II_O$ during immunolabelling had no effect on the observed density of sites containing pol III transcripts (not shown); this suggests that it has no effect on access of the anti-Br-dU to its target. Thus, although these results are consistent with the idea that the active polymerases are found in distinct sites, negative results of this type are never convincing. Indeed, the more co-localized two sites are, the more steric hindrance there is, and the less likely it is that such double-labelling experiments will show it.

More decisive evidence for or against co-localization can be obtained by exploiting steric hindrance between probes (Mason and Williams, 1986). We began by seeing if pre-incubation with anti-pol $II_O$ blocked access of other probes. We found it did not block access of probes directed against pol III protein (Figure 7C, line 1), or its transcripts (Figure 7C, line 3). However, it did block access to half of the sites containing Br-RNA made by pols II + III (Figure 7C, line 2). If: (i) pols II and III were active in spatially separate sites in the ratio 4:1 (Table II); (ii) polymerases and their transcripts were intermingled within a site (so sectioning cannot separate pols from their transcripts); and (iii) the blocking antibody completely prevents access of the anti-Br-dU probe, we would expect 20% of sites to be detected. As 50% of sites are seen, polymerases and their transcripts may not be intermingled (as in both nucleoli and Figure 7A) and/or the blocking antibody might not completely prevent access. These results suggest that pol $II_O$ is found close to its own transcripts, but not to pol III or its transcripts.

We went on to show that pre-incubation with the anti-pol III antibody did not block access of a probe directed against pol $II_O$ protein (Figure 7D, line 4); the two polymerases were in separate places. However, the anti-pol III antibody did prevent access to one-fifth of the sites containing Br-RNA made by both polymerases (Figure 7D, line 5). If we make the assumptions described above, we would expect only four-fifths of the sites to be detected, as observed. We would also expect the anti-pol III antibody to block access to all sites containing Br-RNA made by pol III; however, blocking was incomplete (Figure 7D, line 6), perhaps because polymerases and their transcripts are not completely intermingled (as in Figure 7B). Similar results were obtained using an antibody directed against a different pol III subunit (i.e. RPC53; not shown and Figure 8). These results suggest that pol III is found close to its own transcripts, but not to pol $II_O$ or its transcripts.

Three different approaches described above, i.e. the reduction in site numbers seen when pol III is inhibited (Figures 4 and 5; Table II), the failure to observe significant co-localization of pol $II_O$ with pol III transcripts (not shown) and the more decisive blocking experiments (Figure 7C and D), are all consistent with pols II and III being active in spatially separate sites.

## Discussion

### *Improved conditions for transcription in permeabilized cells*

Sites of nucleoplasmic transcription can be visualized after allowing living or permeabilized cells to extend nascent transcripts in the presence of various precursors (e.g. Br-U, Br-UTP or biotin-CTP), and then immunolabelling the incorporated analogues with fluorochromes or gold particles. The resulting Br-RNA proves not to be spread diffusely throughout euchromatin but is concentrated in discrete sites (see Introduction). As labelling is sensitive to a low concentration of α-amanitin, these mainly represent sites of pol II activity. However, sites of pol III activity have not been detected (Wansink *et al*., 1993; Zeng *et al*., 1997), except in cells infected with adenovirus (Pombo *et al*., 1994). We now describe conditions that preserve sufficient activity and ultrastructure to permit pol III sites to be visualized in uninfected cells.

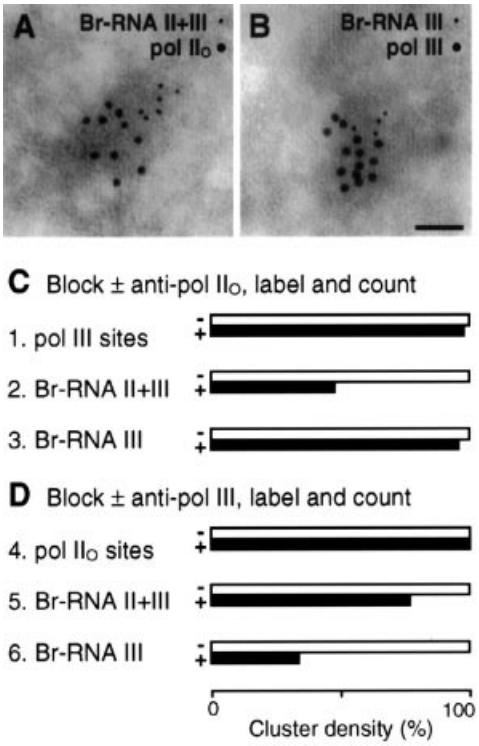


**Fig. 7.** Pol III and its transcripts are found in dedicated sites. Nascent transcripts were extended (100 μM Br-UTP; 15 min) with or without 2 μg/ml α-amanitin; after fixation and cryosectioning, sites containing Br-RNA and pol II$_O$ or pol III were immunolabelled with gold particles and electron micrographs collected. H5 and anti-RPC39 were used to label pol II$_O$ and pol III, respectively (see Figure 8 for a blot illustrating the specificity of the anti-RPC39). For (C) and (D), ⩾30 images from ⩾30 cells were counted; values given by the last 20% analysed changed the progressive mean value of the number of clusters per μm$^2$ by <10%. (**A**) Simultaneous labelling of Br-RNA made by pols II + III (5 nm particles), and pol II$_O$ protein (10 nm particles). (**B**) Simultaneous labelling of Br-RNA made by pol III (5 nm particles) and pol III protein (10 nm particles). Bar = 50 nm. (**C**) Pre-incubation with anti-pol II$_O$ does not block access to sites containing pol III or its transcripts. Cryosections were incubated with or without anti-pol II$_O$, before sites containing pol III or Br-RNA were immunolabelled indirectly with gold particles (5 nm); then, the density of clusters of particles was counted and expressed as a percentage of the value found without anti-pol II$_O$. Line 1: pol III protein. Anti-pol II$_O$ does not block detection of pol III, so the two proteins are in separate places. Line 2: sites containing Br-RNA made by pols II + III. Anti-pol II$_O$ completely blocks access to 48% of the sites containing Br-RNA, so (at least) half contain pol II$_O$. If pols II and III are active in spatially separate sites in the ratio 4:1 (Table II), the polymerases and their transcripts are intermingled within a site, and the blocking antibody completely prevents access of the anti-Br-dU probe, we would expect 20% of sites to be detected. As 48% of sites are seen, the polymerases and their transcripts may not be intermingled (as in A) and/or antibodies may not completely prevent access. Line 3: sites containing Br-RNA made by pol III. Anti-pol II$_O$ does not block access to Br-RNA, showing that the two are in separate places. (**D**) Pre-incubation with anti-pol III blocks access to sites containing pol III transcripts. Cryosections were incubated with or without anti-pol III, before sites containing pol II$_O$ or Br-RNA were immunolabelled indirectly and analysed as in (C). Line 4: pol II$_O$ protein. Anti-pol III does not block detection of pol II$_O$, so the two proteins are in separate places. Line 5: sites containing Br-RNA made by pols II + III. Anti-pol III blocks access to 23% of the sites containing Br-RNA, showing that this fraction of Br-RNA sites contains pol III. This result is consistent with the above assumptions (C, line 2). Line 6: sites containing Br-RNA made by pol III. Anti-pol III blocks access to Br-RNA, showing that the two are in the same places. Inhibition is incomplete, perhaps because the polymerases and their transcripts do not occupy identical regions (as in B).

HeLa cells are lysed with saponin in a 'physiological' buffer containing BSA; then, nascent transcripts are extended in Br-UTP, before the resulting Br-RNA is immunolabelled. Under these conditions, engaged polymerases extend nascent transcripts efficiently (Figure 1A), ultrastructure is preserved (Figure 2) and sites of activity of the four cellular polymerases can be visualized by both light and electron microscopy (Figures 4 and 5). In the absence of any drugs, discrete sites are seen in mitochondria (due to the mitochondrial polymerase), nucleoli (due to pol I) and the nucleoplasm (due to pols II and III).

### *The numbers of engaged pol III complexes*

Several interrelated factors complicate any analysis of pol III activity, which is defined by its insensitivity to moderate concentrations of α-amanitin. First, nascent pol III transcripts are so short (i.e. <250 nucleotides) that they are difficult to label, are easily lost, and are completed so quickly that nascent transcripts exist only fleetingly. Secondly, pol III re-initiates in permeabilized cells, unlike pols I and II. Despite these difficulties, we attempted to estimate the numbers of active pol III complexes in a cell using an approach that relied on the short and discrete length of the major pol III transcripts. After extension in the presence of the inhibitor, tagetitoxin (tagetin), to prevent reinitiation, short pol III transcripts were freed from others by gel electrophoresis; then, we found that ~1400 5S rRNA and ~6500 tRNA transcripts were being made at any moment (Table I). [A typical (tetraploid) HeLa nucleus probably contains roughly this number of 5S and tRNA genes (e.g. Hatlen and Attardi, 1971; Marzluff *et al*., 1974; Sørensen and Frederiksen, 1991). About 2000 5S genes are concentrated in two main loci per haploid genome, with the major one containing >90 genes spread over ~200 kbp (Little and Braaten, 1989; Sørensen and Frederiksen, 1991). Other genes transcribed by pol III include those encoding U6, MRP, 7SK and 7SL RNAs.] As 5S RNA and tRNA are the major transcripts made by pol III (Figure 3A), we conclude that ~10 000 pol III complexes are active at any time, within the range found previously (e.g. Marzluff *et al*., 1974).

### *The size of pol III sites*

We determined the size of pol III sites by immuno-electron microscopy of cryosections. In such thin sections, antibodies have easy access to their targets, and pol III sites become marked by clusters of gold particles. These clusters had a radius of ~20 nm (Figure 6), which we assume is equivalent to that of the underlying complex containing Br-RNA. However, this complex cannot be much larger than the immunogold probe used for analysis, which has a radius of ~10 nm (i.e. a 5 nm gold particle coated by a layer of 3–6 nm of immunoglobulin; Lea and Gross, 1992; Iborra and Cook, 1998); therefore, sizes may be overestimated. A few clusters of clusters were seen that could house nascent RNA transcribed from the repeated genes in the major 5S rRNA locus (Figure 5E).

### *Numbers of sites*

The density of nucleoplasmic sites seen here in two-dimensional images of cryosections is 1.7 times higher than densities seen before (Iborra *et al*., 1996). This probably results partly because many, if not all, pol III

sites were missed before, and partly because the improved approach allows some large sites to be resolved into two or more smaller ones (many clusters of clusters can be seen in Figure 5A). The total number of sites in three-dimensional space can be calculated (using standard stereological procedures) from the numbers and radii of clusters seen in two-dimensional sections (Table II, Figure 6); a typical nucleus contains ~9700 nucleoplasmic sites containing transcripts made by pols II + III, and ~1800 made by pol III.

How accurate is this estimate of the number of active pol III sites? Several reasons make it unlikely that many less active sites go undetected. First, increasing the amount of incorporation 10-fold should raise more of any undetected sites above the threshold of detection, but the increase was only 1.5 times (Table II). Secondly, we might also expect different detection methods to have different thresholds, but light microscopy of whole nuclei or cryosections, and electron microscopy of cryosections gave roughly similar results (Figures 4 and 5; not shown). Thirdly, any undetected sites can contain, in aggregate, only a tiny fraction of the total polymerizing activity. This follows because electron microscopy of cryosections is sufficiently sensitive to detect sites with one-twentieth the average Br-RNA content (in Figure 6, the volume of the smallest sphere detected is one-twentieth of the average), and so one-twentieth the average polymerizing activity. Even if ~10 000 nascent transcripts were housed in the ~1800 sites that are detected, plus another ~8200 that remain unseen, the latter could contribute, at most, only one-fifth of the total activity (because they have $<1/20$ the activity and four times the numbers). Therefore, it seems that most sites are detected. Note that in permeabilized cells, pol III transcripts completed *in vitro* seem unable to move away from the primary transcription site; instead, they accumulate at transcription sites, much like pol II transcripts (Iborra *et al*., 1996).

These results impose constraints on models of pol III transcription. If ~10 000 engaged polymerases are each housed in a distinct site, we have to suggest that there are two distinct populations that differ >20-fold in activity (see above), but there is no evidence for two such populations. However, all results are consistent with ~10 000 nascent pol III transcripts being contained in only ~1800 sites, so that each site would contain approximately five nascent transcripts. As a typical pol III transcription unit can probably accommodate only one polymerase (e.g. Braun *et al*., 1989; Bartholomew *et al*., 1993), each site would then be associated with approximately five templates. Occasional clusters of sites such as those seen in Figure 5E might accommodate 5S transcripts encoded by tandemly repeated genes.

### *Distinct transcription 'factories' containing pols I, II and III*

As each site contains more than one polymerase, we investigated whether pols II and III were each active in their own dedicated sites using three different approaches. In the first, we compared site densities after inhibiting pol II. If the two polymerases were intermingled within a site and if most sites were detected, we would expect inhibition of pol II to have little effect on site density. However, site density fell to one-fifth (Figure 4; Table II), consistent with one-fifth of the sites being dedicated to pol III transcription. The second approach involved seeing if a polymerase was found next to transcripts made by the other enzyme. Although pols II and III often lay immediately next to their own transcripts (Figure 7A and B), they rarely lay next to those made by the other enzyme (not shown). However, such negative results are not decisive, especially when the approach is bedevilled by steric hindrance between immunolabelling probes. Convincing evidence against co-localization was obtained using a third approach that exploited this steric hindrance; cryosections were pre-incubated with an antibody to see if it blocked access of a second. We found that an anti-pol II antibody blocked access to pol II transcripts, but not to pol III protein or its transcripts (Figure 7C); conversely, an anti-pol III blocked access to pol III transcripts, but not to pol II protein or its transcripts (Figure 7D). Therefore, the results of all three approaches were consistent with pols II and III being active in spatially separate sites.

These results suggest that the two nucleoplasmic polymerases, like the nucleolar enzymes, are concentrated in their own dedicated sites. As each site probably contains a number of engaged polymerases, associated templates and transcripts, such sites have been christened transcription 'factories'. Thus, each HeLa cell nucleus would contain a total of ~90 000 nascent transcripts, with ~15 000, ~65 000 and ~10 000 being made by pols I, II and III, respectively (Jackson *et al*., 1998; Table II). It remains to be seen to what extent nucleoplasmic factories resemble those found in nucleoli, but it is attractive to suppose that they share the same basic plan. The nucleolus possesses three major zones (Hozak *et al*., 1994; Shaw and Jordan, 1995): a fibrillar centre (a storage area containing pol I), a dense fibrillar component (where nascent transcripts are found) and a surrounding granular component (where primary transcripts are processed). According to this view, pol II factories would contain a store of enzymes, a zone containing approximately eight nascent transcripts and an adjacent processing area. Analogous pol III factories would be smaller, with only approximately five nascent transcripts. Indeed, the nucleoplasmic polymerases are often found immediately next to their transcripts (Figure 7A and B), which, in turn, are often next to sites rich in processing components (Pombo and Cook, 1996; Iborra *et al*., 1998).

## Materials and methods

### *Buffers, saponin, BSA and inhibitors*

'Physiological buffer' (PB) is 100 mM potassium acetate, 30 mM KCl, 10 mM $Na_2HPO_4$, 1 mM $MgCl_2$, 1 mM $Na_2ATP$ (Sigma Grade I), 1 mM dithiothreitol (DTT) and 0.2 mM phenylmethylsulfonyl fluoride (pH 7.4). As the acidity of ATP batches varies, 100 mM $KH_2PO_4$ (usually ⩽1/100th volume) can be added to adjust the pH. When triphosphates were added to PB, extra $MgCl_2$ was added in an equimolar amount. PB* is PB plus human placental RNase inhibitor (10 U/ml; Amersham). PB-BSA and PB*-BSA contain 100 mg/ml BSA (Sigma A-7030; essentially free of fatty acids and γ-globulin). PBS+ is phosphate-buffered saline (PBS) plus 1% BSA and 0.2% gelatin (from fish skin); where indicated, the pH was adjusted to 8.0. All buffers used up to fixation were ice-cold, unless stated otherwise.

Cells were lysed by addition of a large volume of freshly prepared saponin (Sigma S-7900 or S-4521). Saponin and BSA are mixtures of biomolecules and vary from batch to batch; saponin was titrated to give 95% lysis (assessed by immunofluorescence after Br-UTP incorporation; Figure 4) with each batch of BSA. Saponin (Sigma S-7900) was used for initial experiments (Figures 1, 2 and 4A–H), but a purer form (S-4521)

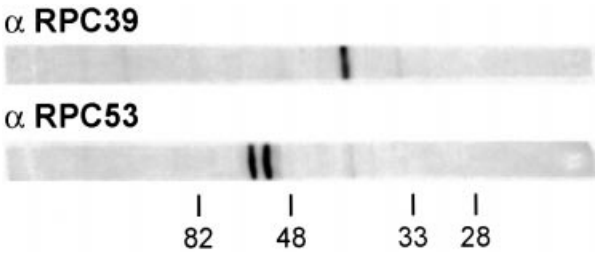


**Fig. 8.** Characterizing anti-pol III antibodies by immunoblotting. A 60 μg aliquot of the proteins in a nuclear extract of HeLa cells was resolved by gel electrophoresis, and RPC39 and RPC53 detected by immunoblotting; photographs of complete lanes from two blots are illustrated. The slowly migrating band detected by anti-RPC53 is probably phosphorylated (not shown).

became available and was used at 0.25 mg/ml for the other figures and the tables. Both forms gave similar results, and higher concentrations of saponin are needed for lysis in BSA. Note that excess saponin can reduce transcriptional activity (e.g. Figure 1, curve 4) largely due to an effect on pol II, so that the proportion of activity due to pol III can increase to 15% (not shown; see also Marzluff *et al*., 1974).

When inhibiting pol I, cells were grown (15 min) in actinomycin D (0.2 μg/ml; Boehringer Mannheim) before lysis. When using α-amanitin (0.001–250 μg/ml; Sigma) or tagetitoxin (tagetin; 20 μM; Cambio), permeabilized cells were incubated for 10 min at 4°C, and then for 5 min at 33°C, before addition of triphosphates to start the reaction.

### *Radiolabelling and analysis of transcripts*

HeLa cells in suspension were grown in [methyl-$^3$H]thymidine (0.2 μCi/ml; ~80 Ci/mmol; Amersham) for ~20 h to label DNA uniformly and allow accurate quantitation of cell number, and then encapsulated ($10^7$/ml), regrown (2 h) and washed once in PBS at 20°C (Jackson and Cook, 1985). One ml of packed agarose beads was resuspended in 10 ml of PB-BSA and saponin, lysed (5 min with intermittent mixing), washed three times in PB-BSA, and the beads were resuspended in an equal volume of PB-BSA. Then 250 μl of packed beads were added to 200 μl of PB*-BSA with or without drugs, incubated (10 min; 4°C), reincubated (5 min; 33°C), and the reactions were started by addition of a 10× concentrate to give final concentrations of 100 μM ATP, CTP and GTP, 5 μM UTP supplemented with a trace of [$^{32}$P]UTP (100 μCi/ml; ~800 Ci/mmol; Amersham), and 1.3 mM $MgCl_2$. For Figure 3 and Table I, 5 μM UTP was replaced by 1–100 μM Br-UTP and a higher concentration of tracer (i.e. 200 μCi/ml). [Addition of Br-UTP had little effect on incorporation due to pol III. In 5 and 100 μM Br-UTP, 4.3% (range 3.7–5.2; $n$ = 5) and 3.5% (range 2.8–4.2; $n$ = 5) of the total intensity in a lane (measured as in Figure 3A) was found in the 5S plus tRNA regions (not shown); this is to be compared with the 4% (range 3.1–5.7; $n$ = 10) of total radioactivity found in all pol III transcripts (determined in 5 μM UTP; Figure 1).] After various times at 33°C, the amount of radiolabel in acid-insoluble material was determined by scintillation counting (Jackson *et al*., 1988).

Transcript profiles were analysed as follows. After transcription, samples were washed three times in PB*-BSA, resuspended in PB*-BSA diluted with 3 vols of 1 mM $MgCl_2$ and 1 mM DTT, and incubated (10 min; 33°C) with 500 U/ml RNase-free DNase and 25 U/ml RNase inhibitor. Next, SDS was added to 0.2%, the agarose was melted (10 min; 75°C) and RNA was purified using RNAzol B (BioGenesis). Then, dried RNA was dissolved in RNase-free water plus 10 U/ml RNase inhibitor, sample buffer containing formamide (Amersham) was added, RNA was denatured (10 min; 75°C), the RNA from equal numbers of cells was run on 6% polyacrylamide 'denaturing' gels (Sambrook *et al*., 1989), and autoradiographic images were collected using a PhosphorImager (Molecular Dynamics). Short transcripts were not lost preferentially during purification as transcript profiles were similar if samples were applied to gels immediately after melting (not shown). The relative intensities in different areas of the autoradiogram were obtained using 'ImageQuaNT' software (Molecular Dynamics) and expressed as a percentage of the total in the lane. The intensities of the bands were obtained after subtracting background measured in adjacent zones (Figure 3A, zones b1–b2).

Examples of calculations used to derive data are as follows. (i) The numbers of nucleotides incorporated into each transcript (from Figure 3A, lane 5). After 30 min elongation in 250 nM [$^{32}$P]UTP (200 μCi/ml) and 100 mM Br-UTP, 100 μl of elongation mixture contained 112 000 and 57 000 acid-insoluble $^3$H and $^{32}$P c.p.m., respectively, or 0.22 $^{32}$P c.p.m./cell (normalized using $^3$H c.p.m./cell), equivalent to 55 pmol of UMP/$10^6$ cells. This is equivalent to $131\times10^6$ nucleotides/cell, as 45S rRNA contains 16% U (DDBJ/EMBL/GenBank accession No. U13369) and constitutes 35% of the total, while other transcripts contain 30% U (Lewin, 1974). If 90 000 polymerases are active per cell and if no polymerases terminate or reinitiate, then each transcript is extended by 1500 nucleotides (Figure 3B). (ii) The numbers of 5S transcripts per cell (from Figure 3A, lane 5). A total of $13\times10^6$ nucleotides of [$^{32}$P]UMP from 400 000 cells (calculated as above) were loaded in a lane. The 5S rRNA region contained 0.56% of the total intensity in the lane after subtracting background. If: (a) 5S rRNA contains 23% U and is 120–121 nucleotides long (corresponding average figures for tRNA are 22% U and 85 nucleotides); (b) a typical transcript is half-complete on lysis, so the other half becomes radiolabelled; and (c) any re-initiated transcripts are fully labelled, it can be calculated that each cell produces 6300 labelled 5S transcripts, of which 1600 were completed during the first (half) cycle (calculated using data from Figure 3A, lane 7). (iii) The number of completed 5S rRNA transcripts per cell (Table I, 100 μM Br-UTP, –tagetin). A total of 57 attomoles of UMP were incorporated into total RNA per cell, and the 5S band contained 0.35% of this; this is equivalent to $0.52\times10^6$ nucleotides/cell, after correcting for the base content of 5S rRNA. In the presence of tagetitoxin, the equivalent figure was $0.08\times10^6$ nucleotides/cell, and, as only half the transcript is labelled, 1400 transcripts are completed *in vitro*. Therefore, $0.43\times10^6$ nucleotides (in 3600 transcripts) are incorporated in subsequent cycles throughout the ~120 nucleotides of the transcripts.

### *Characterization of anti-pol III antibodies*

Two rabbit polyclonal antibodies directed against human RPC39 and RPC53 (Wang and Roeder, 1997) were affinity purified (using RPC39 and RPC53 columns; Harlow and Lane, 1988), and characterized further by immunoblotting as described (Wang and Roeder, 1997) with the following modifications: 60 μg of protein in a HeLa nuclear extract was applied to each lane, the anti-RPC39 and anti-RPC53 were used at 1/1000 dilution and detection was by enhanced chemiluminescence. Figure 8 shows that antibodies were specific as they detect bands of the appropriate size.

### *Microscopy*

For light microscopy of whole cells, sites of transcription were imaged using HeLa cells growing on 13 mm coverslips. Cells were rinsed successively in PBS (20°C) and PB*-BSA, lysed (5 min with intermittent mixing) by addition of saponin in PB*-BSA and rinsed three times in PB*-BSA (BSA was omitted for Figure 2E and F). Coverslips were pre-incubated with or without α-amanitin (35°C; 5 min) in PB*-BSA, and transcription reactions were started by overlaying 150 μl of PB*-BSA with or without α-amanitin supplemented with 100 μM ATP, CTP and GTP, 5 or 100 μM Br-UTP, and 0.305 or 0.4 mM $MgCl_2$ (giving final concentrations of 1.1 mM ATP and 1.305 or 1.4 mM $MgCl_2$). After incubation (35°C), reactions were stopped by rinsing in ice-cold PB*-BSA. Cells were fixed (10 min; 4°C) in 4% paraformaldehyde in 250 mM HEPES buffer (pH 7.4), then in 8% paraformaldehyde in the same buffer (2 h; 4°C), and used for microscopy. For cryosections, cells were treated similarly except that cells were grown in 60 mm Petri dishes, and reactions were carried out by overlaying 3 ml of buffer.

For confocal microscopy of whole cells (Figure 4A–H), free aldehydes were quenched (20 min) in 25 mM glycine in PBS, treated (20 min) with 0.5% Triton X-100 in PBS, washed (five times over 20 min) in PBS, blocked (20 min) with PBS+, and Br-RNA was immunolabelled. Cells were incubated (2 h) with mouse anti-Br-dU antibody (1 μg/ml; clone BMC9318; Boehringer Mannheim) in PBS+ (pH 8.0), washed (eight times over 2 h) in PBS+, and incubated with donkey anti-mouse conjugated with Cy3 (0.5 μg/ml; Jackson Laboratories, multiple-labelling grade). [For all experiments reported here, this anti-Br-dU antibody gave low backgrounds; however, recent batches give high backgrounds, so we now use the analogous antibody produced by clone MD5310 (Caltag Laboratories).] Three-layered sandwiches, using the mouse anti-Br-dU antibody, affinity-purified rabbit anti-mouse IgG (10 μg/ml; Cappel Laboratories) and then a donkey anti-rabbit IgG conjugated with Cy3 (1 μg/ml; Jackson Laboratories, multiple-labelling grade), were also used for increased sensitivity, with similar results (not shown). After immunolabelling, coverslips were rewashed (1 h) in PBS+ and then in PBS–0.1% Tween-20, incubated (10 min) with 20 μM TOTO-3 (Molecular Probes) in PBS–Tween, washed twice in PBS and mounted in Vectashield (Vector Labs). Images were collected on a Bio-Rad MRC

1000/1024 hybrid 'confocal' microscope (running under Comos 7.0a software) using a 0.7 mm aperture, the full dynamic range of grey scale in low scan/low signal mode, and Kalman filtration. Then, images were incorporated into Adobe Photoshop, 'contrast-stretched' and presented without further processing (i.e. without background subtraction). The volume of nucleoplasm (i.e. 660 ± 150 $\mu m^3$; range 424–830; $n = 10$) in permeabilized HeLa cells was determined using Adobe Photoshop from serial optical sections collected at nominal 0.4 μm intervals through whole cells stained with TOTO-3. Each voxel had *x* and *y* dimensions of 45 nm (calibrated according to Bio-Rad's instructions), and a *z* dimension of 0.31 μm and not 0.4 μm (determined by reference to 10 μm latex Nile Red FluoroSpheres from Molecular Probes, as described by Visser *et al*., 1991).

Cryosections were prepared using a modification of existing methods (Tokuyasu, 1980; Griffiths *et al*., 1984; Tooze *et al*., 1991). During fixation in 8% paraformaldehyde, cells were scraped off the surface of the Petri dish and pelleted (200 *g*; 5 min); then, fixation was allowed to continue in the pellet for 20 min before it was dislodged. Next, the pellet was washed in PBS, transferred through three drops of 2.1 M sucrose in PBS over 2 h and then onto a copper block, frozen by immersion in liquid nitrogen, and stored in liquid nitrogen until use. Cryosections (90–150 nm thick, deduced from interference colour) were cut and captured on drops of 2.1 M sucrose in PBS. For light microscopy, sections were transferred to coverslips, quenched with glycine (as above), treated (2 min) with 0.1% Triton X-100 in PBS, washed, blocked, Br-RNA was immunolabelled, and images were collected (all as above, except the first antibody was used at 10 μg/ml). Use of a sheep anti-Br-DNA antibody (1/80; Biodesign International) gave similar results (not shown).

For electron microscopy (Figure 2), fixed cells were post-fixed in reduced osmium tetroxide, contrasted, flat embedded in Epon (Tooze and Hollinshead, 1992) and imaged in a Zeiss EM 912 Omega transmission electron microscope equipped with both conventional, cooled slow-scan CCD (1024×1024 pixels; Proscan) and SIT 66 (Dage-MTI) cameras. For Figure 5, cryosections were cut from the same blocks used for light microscopy, transferred to grids instead of coverslips, quenched, treated with Triton, washed and blocked (all as above). Br-RNA was immunolabelled using the mouse anti-Br-dU antibody (10 μg/ml), washed (as above), incubated (2 h) with immunopurified rabbit anti-mouse IgG (10 μg/ml; Cappel), rewashed, incubated (30 min) with 10% normal goat serum (Jackson Laboratories), and (3–10 h) with goat anti-rabbit IgG conjugated with 5 nm gold particles (1/50; British BioCell) or protein A conjugated with 6 nm gold particles (1/100; prepared as described by Griffiths, 1993). [Two-layered sandwiches, i.e. the mouse anti-Br-dU antibody and goat anti-mouse conjugated with 5 nm gold particles (1/50; British BioCell), led to the detection of only 20% sites (not shown). Four-layered sandwiches, i.e. the mouse anti-Br-dU antibody, rabbit anti-mouse IgG, biotinylated donkey anti-rabbit IgG (5 μg/ml; Jackson Laboratories, multiple-labelling grade) and goat anti-biotin conjugated with 5 nm gold particles (1/50; British BioCell), gave similar cluster densities but higher backgrounds (not shown).] Grids were washed five times over 2–8 h in PBS+, rewashed five times in PBS, fixed (10 min) in 0.5% glutaraldehyde in PBS, washed (eight times) in water, incubated (4°C; 10 min) with 0.3% uranyl acetate in 2% methylcellulose, captured on wire loops, excess methylcellulose blotted on to a filter paper, recovered, and imaged in the electron microscope.

For Figure 7, cryosections were transferred to grids, quenched, treated with Triton, washed, blocked as above and labelled using three antibody layers in various ways. To label Br-RNA and pol $II_O$ (Figure 7A), sections were incubated (2 h) with both mouse anti-Br-dU antibody (10 μg/ml) and the H5 antibody directed against the hyperphosphorylated form of the largest subunit of pol II (1/15 dilution of 'nutridoma' medium; Bregman *et al*., 1995). After washing, they were incubated (2 h) with both rabbit anti-mouse IgG Fc (γ-specific; 1/1500; Cappel) and biotinylated donkey anti-mouse IgM (μ-specific; 5 μg/ml; Jackson Laboratories), washed and incubated (30 min) with 10% normal goat serum (Jackson Laboratories). For the third layer, sections were incubated (3–10 h) with both goat anti-rabbit IgG conjugated with 5 nm gold particles (1/50; British BioCell) and goat anti-biotin conjugated with 10 nm gold particles (1/25; British BioCell), and processed as above. No clusters of 10 nm particles were seen in nucleoli or when the H5 antibody was omitted, and no clusters of 5 nm particles were detected when Br-UTP was omitted from the transcription reaction (not shown). To label Br-RNA and pol III (Figure 7B), sections were incubated (2 h) with both mouse anti-Br-dU antibody (10 μg/ml) and immunopurified rabbit anti-RPC39 antibodies (20 μg/ml; Wang and Roeder, 1997). After washing, they were re-incubated (2 h) with both donkey anti-mouse IgG conjugated with horseradish peroxidase (3 μg/ml; Jackson Laboratories) and biotinylated donkey anti-rabbit IgG (5 μg/ml; Jackson Laboratories), rewashed and incubated (30 min) with 10% normal goat serum. For the third layer, sections were incubated (3–10 h) with goat anti-horseradish peroxidase conjugated with 6 nm gold particles (1/50; Jackson Laboratories) and goat anti-biotin conjugated with 10 nm gold particles (1/25; British BioCell). No clusters of 10 nm particles were seen when the anti-RPC39 antibody was omitted, and no clusters of 5 nm particles were detected when Br-UTP was omitted from transcription reactions (not shown).

For blocking experiments (Figure 7C and D), sections were incubated (2 h) with H5 or anti-RPC39, then (2 h) with H5, anti-RPC39 or mouse anti-Br-dU (all as above). When H5 was followed by anti-RPC39 (Figure 7C, line 1), cryosections were incubated successively with biotinylated donkey anti-rabbit IgG (2 h), normal goat serum (30 min) and goat anti-biotin conjugated with 5 nm gold particles (3–10 h; 1/50; British BioCell). When H5 was followed by anti-Br-dU (Figure 7C, lines 2 and 3), cryosections were incubated successively with rabbit anti-mouse IgG Fc (2 h), normal goat serum (30 min) and goat anti-rabbit IgG conjugated with 5 nm gold particles (3–10 h). When anti-RPC39 was followed by H5 or anti-Br-dU (Figure 7D), sections were incubated successively with biotinylated donkey anti-mouse IgG (2 h; 5 μg/ml; Jackson Laboratories), normal goat serum (30 min) and goat anti-biotin conjugated with 5 nm gold particles (3–10 h). In each case, no sites were detected when the antibody used to detect the target site (e.g. anti-RPC39 for Figure 7C, line 1) was omitted (not shown).

For quantitative analysis, a cluster of gold particles was defined as one containing more than one particle lying within 40 nm of another (centre–centre distance). The radius, *r*, of such clusters was determined after measurement (using SIS 'EsiVision' software supplied with the electron microscope) of the major, 2*x*, and minor, 2*y* (orthoganol), axes of each cluster, from $r = \sqrt{(xy)}$. The average diameter, *D*, of the underlying sites marked by these clusters was determined using the 'sequential subtraction method' (Weibel, 1979, 1980; Pombo *et al*., 1999). The numbers of sites in the three dimensions of a nucleus were calculated as follows (Weibel, 1979): (i) the density ($n_s$) of clusters in two-dimensional images of three-dimensional sections was measured; (ii) the volume density ($n_v$) was calculated using Abercrombie's formula $n_v = n_s/(D + T)$, where *T* is the section thickness; and (iii) the number of sites per nucleus were calculated with knowledge of the nuclear volume. Calculated values in three-dimensional space are sensitive both to values of site radius and to nucleoplasmic volume.

## Acknowledgements

We thank S.L.Warren for the H5 antibody, E.M.M.Manders, J.Bartlett and J.Sanderson for their help, and Fundaçao para a Ciencia e a Tecnologia (Program Praxis XXI; Portugal), the Royal Society, Cancer Research Campaign, Wellcome Trust and NIH (grant CA42567) for support.

## References

Bartholomew,B., Durkovich,D., Kassavetis,G.A. and Geiduschek,P.E. (1993) Orientation and topography of RNA polymerase III in transcription complexes. *Mol. Cell. Biol.*, **13**, 942–952.

Braun,B.R., Riggs,D.L., Kassavetis,G.A. and Geiduschek,E.P. (1989) Multiple states of protein–DNA interaction in the assembly of transcription complexes on *Saccharomyces cerevisiae* 5S ribosomal RNA genes. *Proc. Natl Acad. Sci. USA*, **86**, 2530–2534.

Bregman,D.B., Du,L., van der Zee,S. and Warren,S.L. (1995) Transcription-dependent redistribution of the large subunit of RNA polymerase II to discrete nuclear domains. *J. Cell Biol.*, **129**, 287–298.

Chambon,P. (1974) RNA polymerases. In Boyer,P.D. (ed.), *The Enzymes*. Academic Press, New York, NY, Vol. 10, pp. 261–331.

Dahmus,M.E. (1996) Reversible phosphorylation of the C-terminal domain of RNA polymerase II. *J. Biol. Chem.*, **271**, 19009–19012.

Fakan,S. (1994) Perichromatin fibrils are *in situ* forms of nascent transcripts. *Trends Cell Biol.*, **4**, 86–90.

Fakan,S. and Puvion,E. (1980) The ultrastructural visualization of nuclear and extranucleolar RNA synthesis and distribution. *Int. Rev. Cytol.*, **65**, 255–299.

Fakan,S., Puvion,E. and Spohr,G. (1976) Localization and characterization of newly synthesized nuclear RNA in isolated rat hepatocytes. *Exp. Cell Res.*, **99**, 155–164.

Fay,F.S., Taneja,K.L., Shenoy,S., Lifshitz,L. and Singer,R.H. (1997) Quantitative digital analysis of diffuse and concentrated nuclear distributions of nascent transcripts, SC35 and poly(A). *Exp. Cell Res.*, **231**, 27–37.

Geiduschek,E.P. and Tocchini-Valentini,G.P. (1988) Transcription by RNA polymerase III. *Annu. Rev. Biochem.*, **57**, 873–914.

Grande,M.A., van der Kraan,I., de Jong,L. and van Driel,R. (1997) Nuclear distribution of transcription factors in relation to sites of transcription and RNA polymerase II. *J. Cell Sci.*, **110**, 1781–1791.

Griffiths,G. (1993) *Fine Structure Immunocytochemistry.* Springer-Verlag, Berlin/Heidelberg, Germany.

Griffiths,G., McDowall,A., Back,R. and Dubochet,J. (1984) On the preparation of cryosections for immunocytochemistry. *J. Ultrastruct. Res.*, **89**, 65–78.

Harlow,E. and Lane,D. (1988) *Antibodies: A Laboratory Manual*. Cold Spring Harbor Laboratory Press, Cold Spring Harbor, NY.

Hatlen,L. and Attardi,G. (1971) Proportion of the HeLa cell genome complementary to transfer RNA and 5S RNA. *J. Mol. Biol.*, **56**, 535–553.

Hozak,P., Cook,P.R., Schofer,C., Mosgoller,W. and Wachtler,F. (1994) Site of transcription of ribosomal RNA and intra-nucleolar structure in HeLa cells. *J. Cell Sci.*, **107**, 639–648.

Iborra,F.J. and Cook,P.R. (1998) The size of sites containing SR proteins in human nuclei: problems associated with characterizing small structures by immunogold labelling. *J. Histochem. Cytochem.*, **46**, 985–992.

Iborra,F.J., Pombo,A., Jackson,D.A. and Cook,P.R. (1996) Active RNA polymerases are localized within discrete transcription 'factories' in human nuclei. *J. Cell Sci.*, **109**, 1427–1436.

Iborra,F.J., Jackson,D.A. and Cook,P.R. (1998) The path of transcripts from extra-nucleolar synthetic sites to nuclear pores: transcripts in transit are concentrated in discrete structures containing SR proteins. *J. Cell Sci.*, **111**, 2269–2282.

Jackson,D.A. and Cook,P.R. (1985) Transcription occurs at a nucleoskeleton. *EMBO J.*, **4**, 919–925.

Jackson,D.A., Yuan,J. and Cook,P.R. (1988) A gentle method for preparing cyto- and nucleo-skeletons and associated chromatin. *J. Cell Sci.*, **90**, 365–378.

Jackson,D.A., Hassan,A.B., Errington,R.J. and Cook,P.R. (1993) Visualization of focal sites of transcription within human nuclei. *EMBO J.*, **12**, 1059–1065.

Jackson,D.A., Iborra,F.J., Manders,E.M.M. and Cook,P.R. (1998) Numbers and organization of RNA polymerases, nascent transcripts and transcription units in HeLa nuclei. *Mol. Biol. Cell*, **9**, 1523–1536.

Kim,E., Du,L., Bregman,D.B. and Warren,S.L. (1997) Splicing factors associate with hyperphosphorylated RNA polymerase II in the absence of pre-mRNA. *J. Cell Biol.*, **136**, 19–28.

Kock,J. and Cornelissen,R.W. (1991) Characterization of the RNA polymerases of *Crithidia fasciculata*. *Mol. Microbiol.*, **5**, 835–842.

Kovelman,R. and Roeder,R.G. (1990) Sarkosyl defines three intermediate steps in transcription initiation by RNA polymerase III: application to stimulation of transcription by E1A. *Genes Dev.*, **4**, 646–658.

Lea,P. and Gross,D.K. (1992) Effective diameters of protein A–gold and goat anti-rabbit–gold conjugates visualized by field emission scanning electron microscopy. *J. Histochem. Cytochem.*, **40**, 751–758.

Lewin,B. (1974) *Gene Expression—2: Eukaryotic Chromosomes*. Vol. II, Wiley, London, UK.

Little,R.D. and Braaten,D.C. (1989) Genomic organization of human 5S rRNA and sequence of one tandem repeat. *Genomics*, **4**, 376–383.

Maraia,R.J., Kenan,D.J. and Keene,J.D. (1994) Eukaryotic transcription termination factor La mediates transcript release and facilitates reinitiation by RNA polymerase III. *Mol. Cell. Biol.*, **14**, 2147–2158.

Marzluff,W.F., Murphy,E.C. and Huang,R.C.C. (1974) Transcription of the genes for 5S ribosomal RNA and transfer RNA in isolated mouse myeloma cell nuclei. *Biochemistry*, **13**, 3689–3696.

Mason,D.W. and Williams,A.F. (1986) Kinetics of antibody reactions and the analysis of cell surface antigens. In Weir,D.M. (ed.), *Handbook of Experimental Immunobiology.* Blackwell Scientific Publications, Oxford, UK, pp. 38.1–38.17.

Matera,A.G. and Ward,D.C. (1993) Nucleoplasmic organization of small nuclear ribonucleoproteins in cultured human cells. *J. Cell Biol.*, **121**, 715–727.

Matera,A.G., Frey,M.R., Margelot,K. and Wolin,S.L. (1995) A perinucleolar compartment contains several RNA polymerase III transcripts as well as the polypyrimidine tract-binding protein, hnRNP I. *J. Cell Biol.*, **129**, 1181–1193.

McReynolds,L. and Penman,S. (1974) A polymerase activity forming 5S and pre-4S RNA in isolated HeLa cell nuclei. *Cell*, **1**, 139–145.

Pawley,J.B. (1995) Fundamental limits of confocal microscopy. In Pawley,J.B. (ed.), *Handbook of Biological Confocal Microscopy.* Plenum Press, New York, NY, pp. 373–387.

Pombo,A. and Cook,P.R. (1996) The localization of sites containing nascent RNA and splicing factors. *Exp. Cell Res.*, **229**, 201–203.

Pombo,A., Ferreira,J., Bridge,E. and Carmo-Fonseca,M. (1994) Adenovirus replication and transcription sites are spatially separated in the nucleus of infected cells. *EMBO J.*, **13**, 5075–5085.

Pombo,A., Cuello,P., Schul,W., Yoon,J.-B., Roeder,R.G., Cook,P.R. and Murphy,S. (1998) Regional and temporal specialization in the nucleus: a transcriptionally active nuclear domain rich in PTF, Oct1 and PIKA antigens associates with specific chromosomes early in the cell cycle. *EMBO J.*, **17**, 1768–1778.

Pombo,A., Hollinshead,M. and Cook,P.R. (1999) Bridging the resolution gap: imaging the same transcription factories in cryosections by light and electron microscopy. *J. Histochem. Cytochem.*, **47**, 471–480.

Sambrook,J., Fritsch,E.F. and Maniatis,T. (1989) *Molecular Cloning: A Laboratory Manual*. Cold Spring Harbor Laboratory Press, Cold Spring Harbor, NY.

Shaw,P.J. and Jordan,E.G. (1995) The nucleolus. *Annu. Rev. Cell Dev. Biol.*, **11**, 93–121.

Sørensen,P.D. and Frederiksen,S. (1991) Characterization of human 5S rRNA genes. *Nucleic Acids Res.*, **19**, 4147–4151.

Steinberg,T.H. and Burgess,R.R. (1992) Tagetitoxin inhibition of RNA polymerase III transcription results from enhanced pausing at discrete sites and is template-dependent. *J. Biol. Chem.*, **267**, 20204–20211.

Steinberg,T.H., Mathews,D.E., Durbin,R.D. and Burgess,R.R. (1990) Tagetitoxin: a new inhibitor of eukaryotic transcription by RNA polymerase III. *J. Biol. Chem.*, **265**, 499–505.

Tokuyasu,K.T. (1980) Immunochemistry on ultrathin frozen sections. *Histochem. J.*, **12**, 381–403.

Tooze,J. and Hollinshead,M. (1992) In AtT20 and HeLa cells brefeldin A induces the fusion of tubular endosomes and changes their distribution and some of their endocytic properties. *J. Cell Biol.*, **118**, 813–830.

Tooze,J., Hollinshead,M., Hensel,G., Kern,H.F. and Hoflack,B. (1991) Regulated secretion of mature cathepsin B from rat exocrine pancreatic cells. *Eur. J. Cell. Biol.*, **56**, 187–200.

Udvardy,A. and Seifart,K.H. (1976) Transcription of specific genes in isolated nuclei from HeLa cells *in vitro*. *Eur. J. Biochem.*, **62**, 353–363.

Visser,T.D., Oud,J.L. and Brakenhoff,G.J. (1991) Refractive index and axial distance measurements in 3D microscopy. *Optik*, **90**, 17–19.

Wang,Z. and Roeder,R.G. (1997) Three human RNA polymerase III-specific subunits form a subcomplex with a selective function in specific transcription initiation. *Genes Dev.*, **11**, 1315–1326.

Wansink,D.G., Schul,W., van der Kraan,I., van Steensel,B., van Driel,R. and de Jong,L. (1993) Fluorescent labelling of nascent RNA reveals transcription by RNA polymerase II in domains scattered throughout the nucleus. *J. Cell Biol.*, **122**, 283–293.

Weibel,E.R. (1979) *Stereological Methods: Practical Methods for Biological Morphometry.* Vol. 1. Academic Press, London, UK.

Weibel,E.R. (1980) *Stereological Methods: Theoretical Foundations*. Vol. 2. Academic Press, London, UK.

Weil,P.A. and Blatti,S.P. (1976) HeLa cell deoxyribonucleic acid dependent RNA polymerases: function and properties of the class III enzymes. *Biochemistry*, **15**, 1500–1509.

Weinmann,R., Raskas,H.J. and Roeder,R.G. (1975) The transcriptional role of host DNA-dependent RNA polymerases in adenovirus-infected KB cells. *Cold Spring Harbor Symp. Quant. Biol.*, **34**, 495–500.

Zeng,C., Kim,E., Warren,S.L. and Berget,S.M. (1997) Dynamic relocation of transcription and splicing factors dependent upon transcriptional activity. *EMBO J.*, **16**, 1401–1412.

*Received January 7, 1999; revised and accepted February 23, 1999*